Transcriptomic and cellular decoding of functional brain connectivity changes reveal regional brain vulnerability to pro- and anti-inflammatory therapies

D. Martins[a#], O. Dipasquale[a], K. Davies[b,c], E. Cooper[1], J. Tibble[d], M. Veronese[a,e], M. Frigo[f], S.C.R. Williams[a], F. Turkheimer[a], M. Cercignani[g], N.A. Harrison[g,h#]

[a]Department of Neuroimaging, Institute of Psychiatry, Psychology and Neuroscience, King's College London, De Crespigny Park, London SE5 8AF, UK.

[b]Department of Neuroscience, Brighton and Sussex Medical School, University of Sussex Campus, Brighton BN1 9RY, UK.

[c]Department of Rheumatology, Brighton & Sussex University Hospitals, Brighton, UK.

[d]Department of Hepatology, Brighton & Sussex University Hospitals, Brighton, UK.

[e]Department of Information Engineering, University of Padua, Padua, Italy.

[f]Université Côte d'Azur, INRIA, France.

[g]Cardiff University Brain Research Imaging Centre, Cardiff University, Cardiff CF24 4HQ, UK.

[h]Department of Neuroscience, Brighton and Sussex Medical School, University of Sussex Campus, Brighton, BN1 9RY, UK.

[#]Corresponding authors:

Daniel Martins, MD PhD

Department of Neuroimaging,

Institute of Psychiatry, Psychology and Neuroscience, King's College London

De Crespigny Park, London SE5 8AF, United Kingdom

Email: daniel.martins@kcl.ac.uk

Telephone: +44 (0)2032283064

Neil Harrison MBBS PhD MRCP MRCPsych

Cardiff University Brain Research Imaging Centre (CUBRIC)

Maindy Road, Cardiff, CF24 4HQ

Division of Psychological Medicine and Clinical Neuroscience

Email: HarrisonN4@cardiff.ac.uk

Telephone: 02920 876785 (ext 76785)

Category of manuscript

Original research

Abstract

Background: Systemic inflammation induces acute changes in mood, motivation and cognition that closely resemble those observed in depressed individuals. However, the mechanistic pathways linking peripheral inflammation to depression-like psychopathology via intermediate effects on brain function remain incompletely understood.

Methods: We combined data from 30 patients initiating interferon-α treatment for Hepatitis-C and 20 anti-tumour necrosis factor (TNF) therapy for inflammatory arthritis and used resting-state functional magnetic resonance imaging to investigate acute effects of each treatment on regional global brain connectivity (GBC). We leveraged transcriptomic data from the Allen Human Brain Atlas to uncover potential biological and cellular pathways underpinning regional vulnerability to GBC changes induced by each treatment.

Results: Interferon-α and anti-TNF therapies both produced differential small-to-medium sized decreases in regional GBC. However, these were observed within distinct brain regions and the regional patterns of GBC changes induced by each treatment did not correlate suggesting independent underlying processes. Further, the spatial distribution of these differential GBC decreases could be captured by multivariate patterns of constitutive regional expression of genes respectively related to: i) neuroinflammation and glial cells; and ii) glutamatergic neurotransmission and neurons. The extent to which each participant expressed patterns of GBC changes aligning with these patterns of transcriptomic vulnerability also correlated with both acute treatment-induced changes in interleukin-6 (IL-6) and, for Interferon-α, longer-term treatment-associated changes in depressive symptoms.

Conclusions: Together, we present two transcriptomic models separately linking regional vulnerability to the acute effects of interferon-α and anti-TNF treatments on brain function to glial neuroinflammation and glutamatergic neurotransmission. These findings generate hypotheses about two potential brain mechanisms through which bidirectional changes in peripheral inflammation may contribute to the development/resolution of psychopathology.

Key-words: Depression; Interferon-α; anti-TNF; global brain connectivity; Transcriptomic vulnerability; Imaging transcriptomics.

Introduction

Inflammation is increasingly recognized as an aetiological factor in several neuropsychiatric disorders(1-4) with arguably the most robust empirical evidence being the association with major depressive disorder (MDD)(5). For instance, patients with MDD show activated inflammatory pathways in both the blood(6) and cerebrospinal fluid (CSF)(7, 8). Patients with chronic Hepatitis-C infection or melanoma treated with interferon-α develop depressive symptoms, which evolve over time to appear clinically indistinguishable from MDD(9-11). Conversely, patients with pro-inflammatory diseases such as rheumatoid arthritis experience a high burden of depressive symptoms, that improve following suppression of peripheral inflammation with anti-Tumour Necrosis Factor (anti-TNF) therapies (11-13). Patients with treatment-resistant depression in the context of raised peripheral inflammatory markers have also been shown to improve clinically following treatment with the cytokine blocking agent infliximab(14). Collectively, these findings provide compelling evidence that activation of the immune system is causally associated with depressive symptoms. This causal association implicates intermediate effects of peripheral inflammation on the brain(15). However, the mechanistic pathways underpinning these effects remain uncertain.

In attempts to bridge this gap, functional magnetic resonance imaging (fMRI) studies have investigated the relationship between peripheral inflammation and brain function, both at rest (resting-state fMRI) and during specific affective and cognitive paradigms (task-based fMRI)(15). The vast majority have taken a cross-sectional approach, correlating peripheral inflammatory markers with neural activity. A smaller number have sought to test a causal relationship by using an experimental approach, e.g. by collecting fMRI data before and after a planned inflammatory challenge, such as administration of interferon-α to hepatitis patients(16), or typhoid vaccine(17, 18) and lipopolysaccharide(19) to healthy volunteers. Collectively, these experimental studies have provided robust evidence that peripheral inflammation can cause changes in brain function within a discrete set of cortical and sub-cortical structures, such the amygdala, hippocampus, hypothalamus, striatum, insula, midbrain, and brainstem, as well as prefrontal and temporal

cortices(15). Together, these studies broadly support the concept of “inflammation vulnerable” areas or networks in the human brain, many of which have also been reported to show depression-related differences in functional responses and/or connectivity in case-control fMRI studies of MDD patients(20-22). However, it remains unclear what biological factors underpin this regional vulnerability making it difficult to develop precise neurobiological models of how inflammation perturbs brain function and behaviour, and ultimately identify potential pathways amenable to pharmacological intervention.

To a large extent, this absence of precise regional vulnerability models of inflammation-induced changes in brain function reflects the lack of specificity of conventional fMRI-based analytic techniques to the underlying molecular and cellular properties of brain tissue(23). The recent introduction of comprehensive, brain-wide gene expression atlases such as the Allen Human Brain Atlas (AHBA) has opened new opportunities for understanding how spatial variations in macroscopic neuroimaging phenotypes relate to underlying molecular differences at the transcriptomic scale (24, 25). This approach, which relies on identifying genes with spatial profiles of regional expression that track anatomical variations in a particular neuroimaging phenotype, has begun to provide insights into how regional variations in gene expression relate to diverse properties of brain structure(26-31), function(32-38) and neurochemistry(39), and how these change during brain disease(40-50) and development(51-53).

Here, we explored the potential biological and cellular transcriptomic pathways underpinning regional vulnerability to changes in resting brain function after pro- (interferon-α) and anti-inflammatory (anti-TNF) therapies. We pooled data from a previous study including repeat scanning from 30 patients initiating interferon-α treatment for Hepatitis-C and 20 patients initiating anti-TNF therapy for inflammatory arthritis. We acquired clinical, cytokine and resting-state fMRI data before and after each treatment to investigate acute effects of pro/anti-inflammatory therapies on regional global brain connectivity (GBC). In contrast to task-based fMRI, use of resting-state fMRI (rs-fMRI) allowed us to uncover basic pharmacological mechanisms that are not restricted to circuits engaged by any specific paradigm(54) and provide a more accurate picture of regional brain vulnerability to treatment-induced functional changes.

We hypothesized that interferon-α and anti-TNF treatments would result in divergent changes in GBC across the whole-brain (and predicted that the spatial patterns of changes would at least partially anti-correlate). Based on current models which posit that peripheral inflammation influences the brain by engaging local neuroinflammatory processes(55), we also hypothesized that the extent to which the GBC of a brain region in-/decreased in response to these treatments could be explained by spatial variation in the distribution of genes of the neuroimmune axis, such as those expressed in microglia and astrocytes, in the healthy human brain. This same model also predicted that inter-individual differences in peripheral inflammation (and their expression as depressive symptoms) should therefore influence the extent to which each subject manifested patterns of GBC changes resembling the distribution of these neuroimmune genes.

Materials and Methods

Participants

Thirty-three individuals (23 male, mean 48.4 ± 10.7 years) were recruited before initiating interferon-α therapy for Hepatitis-C and 30 (10 male, mean 50.4 ± 15.7 years) before initiating anti-TNF therapy for inflammatory arthritis (25 Rheumatoid arthritis, 2 Psoriatic Arthritis, 3 Ankylosing spondylitis) as previously reported(11). All were fluent in English and fulfilled National Institute for Health and Care Excellence (NICE) guidelines for starting interferon-α-based therapy or anti-TNF therapy. Inclusion and exclusion criteria can be found in the Supplementary Information (SI). The study was approved by Cambridge Central (12/ EE/0491) and South East Coast (11/LO/1320) National Research Ethics Committees. All subjects provided written informed consent. Data from a subsample of our interferon-α dataset has been previously published as part of *Dipasquale et al.* (2016)(16) and *Davies et al.*, 2020(11).

Study design

MRI acquisition followed by blood sampling was performed at baseline and after the first interferon-α (4 h) or anti-TNF (24 h) injection, timed to coincide with reported onset of subjective effects and preclinical data confirming actions of interferon-α and anti-TNF on the brain at these timepoints(56-59). Complete rs-fMRI data was available for both MRI sessions for all interferon-

α treated patients and 24 anti-TNF treated patients. After excluding three interferon-α treated patients and four anti-TNF treated patients because of excessive head movement (mean framewise displacement > 0.25 mm) during one of the two sessions, our final sample consisted of 30 interferon-α and 20 anti-TNF treated patients. Inflammatory response and depressive symptoms were evaluated at each MRI visit and after 12 weeks of therapy in all participants. Interferon-α treated patients underwent additional behavioural assessments at 4 and 8 weeks to capture the more rapid symptom evolution in this group (Figure 1). Further details on clinical assessments can be found in the SI.

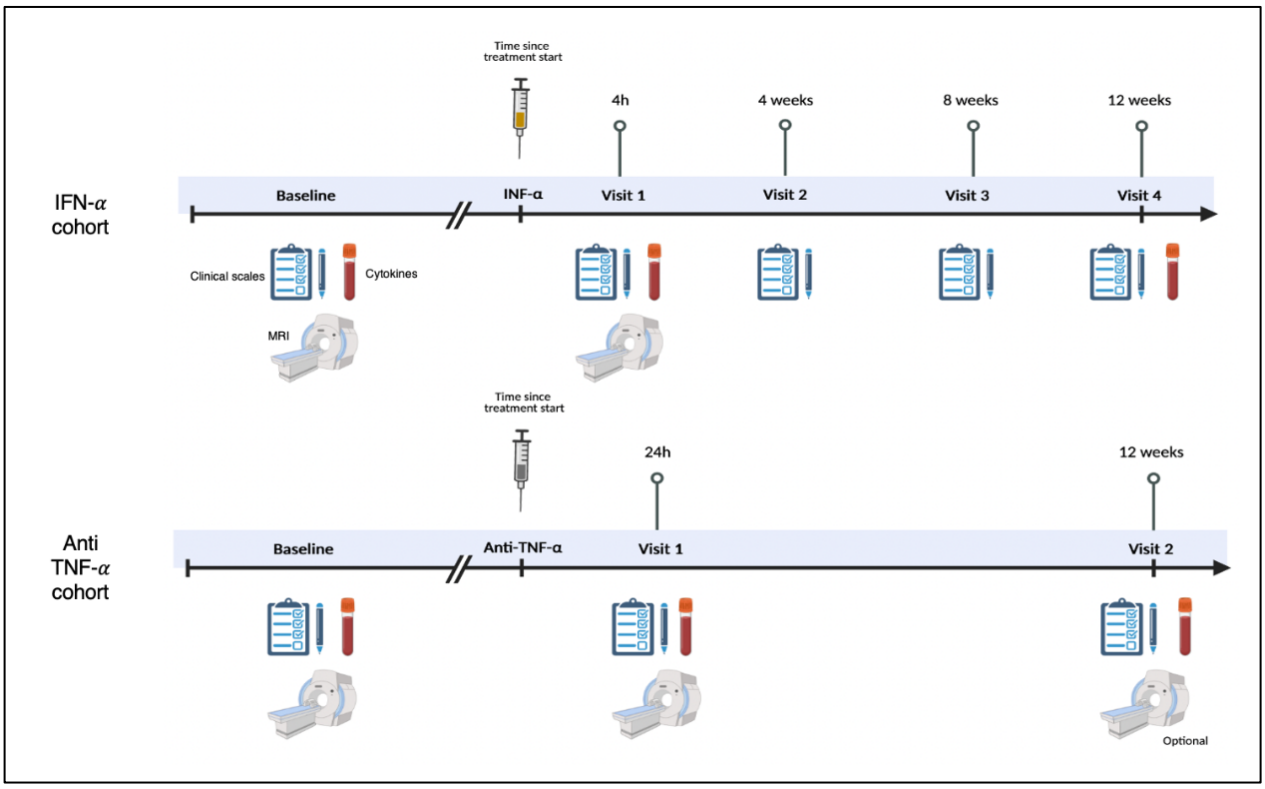

Figure 1. Design and protocol. Figure summarizing the study design and data collection in each cohort. Data collection followed slightly different protocols between cohorts, to align with timescales of subjective responses to treatment and clinical follow-up schedules. The diagram provides a summary of the types of data (MRI, clinical scales, cytokines) collected at each visit.

Image acquisition

MR imaging was performed on a 1.5T Siemens Avanto (Siemens AG Medical Solutions, Erlangen, Germany) equipped with a 32-channel head-coil. Functional MRI data were obtained during rest using a T2*-weighted EPI sequence (TR/TE = 2520/43 ms; flip angle=90°; resolution=3×3×3 mm, with 20% between-slice gap; matrix size=64x64; 34 axial slices; 190 volumes). Functional data for four anti-TNF treated patients were acquired with a slightly longer TR (2620ms) and consequently a slightly smaller number of volumes (180) to maintain the total duration the same. Excluding these four patients did not significantly change our estimates of treatment-induced changes in GBC; therefore, we kept these patients in all analyses to maximize power. A 3D T1-weighted anatomical scan was obtained for each participant in one session using an MPRAGE acquisition (TR=2730ms, TE=3.57ms, TI=1000ms, flip angle=7°).

Imaging analysis

The interferon-α and anti-TNF rs-fMRI datasets were pre-processed using the FMRIB Software Library (FSL). Pre-processing steps included volume re-alignment with MCFLIRT(60), non-brain tissue removal with the brain extraction tool (BET)(61), spatial smoothing with an 8-mm FWHM Gaussian kernel and de-noising with ICA-based Automatic Removal Of Motion Artifacts (ICA-AROMA)(62). Additionally, subject-specific WM and CSF masks, obtained from the segmentation of the subjects' structural images and eroded to minimize the contribution of grey matter partial volume effects, were used to extract and regress out the mean WM and CSF signals from each participant's pre-processed dataset. A high-pass temporal filter with a cut-off frequency of 0.005 Hz was also applied.

A study-specific template representing the average T1-weighted anatomical image across subjects was built using the Advanced Normalization Tools (ANTs)(63). Each participant's dataset was co-registered to its corresponding structural scan, then normalized to the study-specific template before warping to standard MNI152 space then images resampled at 2 mm^3 resolution.

Global Brain Connectivity analysis

Changes in global brain connectivity (GBC) to each treatment was used as the primary outcome (dependent) variable as it has been shown to be exquisitely sensitive to the effects of pharmacological manipulations in humans(64). GBC was estimated with an in-house Python script (version 1)(65). Briefly, for each scan, we estimated the mean time series across all voxels of each of the 83 regions of interest (ROIs) of the Desikan-Killiany (DK) atlas(66) then computed pairwise Pearson's correlation between the mean time series of all pairs of regions. Finally, we averaged all positive correlations to produce a single summary value (we kept all positive correlations without applying any threshold). These values were transformed to Fisher's Z values and projected onto the corresponding DK regions in atlas space to generate GBC maps. Following previous recommendations, we excluded all negative correlations when calculating the GBC due to poor understanding of the biological meaning of negative correlations(67-69). The python script can be downloaded from https://github.com/matteofrigo/gfcpy.

We then investigated treatment effects by comparing baseline and post-administration GBC for each region using paired-T tests, applying false discovery rate (FDR) correction for the total number of regions tested.

Microarray expression data - Allen Human Brain Atlas (AHBA): Regional microarray expression data were obtained from the six post-mortem brains provided by the Allen Human Brain Atlas (AHBA; http://human.brain-map.org/) (ages 24–57 years)(70). The *abagen* toolbox (https://github.com/netneurolab/abagen) was used to process and map the transcriptomic data to the 83 parcellated regions of the DK brain atlas(66). Briefly, genetic probes were reannotated using information provided by *Arnatkeviciute et al.* (71) instead of the default probe information from the AHBA dataset, hence discarding probes that cannot be reliably matched to genes. Following previously published guidelines for probe-to-gene mappings and intensity-based filtering(71), the reannotated probes were filtered based on their intensity relative to background noise level; probes with intensity lower than the background in ≥50% of samples were discarded. A single probe with the highest differential stability (highest pooled correlation across donors)

was selected to represent each gene(72). This procedure retained 15,633 probes, each representing a unique gene. Differential stability was calculated as(72):

$$\Delta_S(p) = \frac{1}{\binom{N}{2}} \sum_{i=1}^{N-1} \sum_{j=i+1}^{N} \rho[B_i(p), B_j(p)]$$

Here, ρ is Spearman's rank correlation of the expression of a single probe *p* across regions in two donor brains, Bi and Bj, and *N* is the total number of donor brains. This procedure retained 15,633 probes, each representing a unique gene.

Next, tissue samples were assigned to brain regions using their corrected MNI coordinates (https://github.com/chrisfilo/alleninf) by finding the nearest region within a radius of 2 mm. To reduce the potential for misassignment, sample-to-region matching was constrained by hemisphere and cortical/subcortical divisions. If a brain region was not assigned to any sample based on the above procedure, the sample closest to the centroid of that region was selected to ensure that all brain regions were assigned a value. Samples assigned to the same brain region were averaged separately for each donor. Gene expression values were then normalized separately for each donor across regions using a robust sigmoid function and rescaled to the unit interval. We applied this procedure for cortical and subcortical regions separately, as suggested by *Arnatkeviciute et al.* **(71)**. Scaled expression profiles were finally averaged across donors, resulting in a single matrix with rows corresponding to brain regions and columns corresponding to the retained 15,633 genes.

As the AHBA currently includes right hemisphere data for only two subjects, we only considered transcriptomic data from the left hemisphere (34 cortical + 7 subcortical regions). Nevertheless, for the imaging transcriptomics analyses, instead of considering GBC changes from the left hemisphere alone, we averaged the T-statistics for each cortical and subcortical region across both hemispheres to avoid discarding data from the right hemisphere and account for asymmetry of effects between hemispheres.

Imaging transcriptomics: Partial least square regression (PLS) was used to investigate associations between treatment-induced GBC changes and brain gene expression (47). This approach ranks all genes by their multivariate spatial alignment with GBC changes induced by each treatment. The first PLS component (PLS_1) is the linear combination of the weighted gene expression scores that have a brain expression map that covaries most closely with the map of GBC changes. As components are calculated to explain the maximum covariance between the dependent and independent variables, the first component does not necessarily explain the maximum variance in the dependent variable. However, as the number of components calculated increases, they tend to progressively explain less variance in the dependent variable. Here, we tested across a range of components (between 1 and 15) and quantified the relative variance explained by each component. The statistical significance of the variance explained by each component was tested by permuting the response variables 1,000 times, while accounting for spatial autocorrelation (see section "Spatial permutation test (spin test)" below). We focussed our subsequent analyses on the component explaining the greatest variance, which in our case was always the first component (PLS_1). Error in estimating each gene's PLS_1 weight was assessed by bootstrapping (resampling with replacement of the 41 brain regions), and the ratio of the weight of each gene to its bootstrap standard error was used to calculate the *Z* scores and, hence, rank the genes according to their contribution to PLS_1(73). The code used to implement these analyses was adapted from https://github.com/SarahMorgan/Morphometric_Similarity_SZ.

Ensemble gene set enrichment analyses: We then used the list of genes ranked by their respective weights in the PLS_1 component to perform enrichment analyses for biological pathways (gene ontology - GO) and genes expressed in different brain cell types, as identified in previous single-cell transcriptomic studies of the human brain(74-78). These analyses were implemented using the ensemble enrichment analysis toolbox of Fulcher et al. (https://github.com/benfulcher/GeneSetEnrichmentAnalysis)(79). Significance was assessed against ensembles of 10,000 randomized brain markers where the brain's spatial autocorrelation was preserved (see below) enabling us to determine whether a given brain phenotype is

significantly correlated to genes in a category beyond what would be expected from the null phenotypes and minimise the risk of false positives(79).

Spatial permutation test (spin test): Several of our analyses required the generation of randomized nulls of brain maps. To account for the inherent spatial autocorrelation of the imaging data, we relied on spatial autocorrelation-preserving spin rotations of our imaging maps. This was performed using the *Vasa* method as implemented in previous studies (80-83). Note that in this method, parcels are reassigned without consideration for the medial wall or its rotated location. Since subcortical regions cannot be projected onto the inflated spherical pial surface (which is a requirement for the creation of spin rotations), we incorporated the subcortex into our null models by shuffling the seven subcortical regions with respect to one another, whereas the cortical regions were shuffled using the spin rotations.

Cytokine analyses

Blood (20 mL) was drawn into Vacutainer tubes containing ethylenediaminetetraacetic acid (EDTA) anticoagulant, centrifuged at 1300 rpm for 10 min and plasma was removed, aliquoted, and frozen at −80 °C before analysis. Interleukin-6 (IL-6), Tumor Necrosis factor (TNF), IL-10 and IL-1 Receptor antagonist (IL-1Ra) Quantikine® ELISAs (R&D Systems, Abingdon, UK), as described in further detail in Davies et al., 2020 (11). Cytokines were selected to provide an index of both pro- and anti-inflammatory responses.

Correlations with changes in peripheral inflammation markers and symptoms: We next investigated whether the physical manifestation of topographic PLS_1 maps was related to interindividual differences in changes in peripheral inflammatory markers and depression/fatigue symptoms. For each participant, we first calculated a map of treatment-induced GBC changes (by subtracting the individual's post-administration and baseline maps) then correlated this with the regional PLS_1 scores map. This resulted in a distribution of correlations that describes how well an individual manifests the gene score pattern. This vector of correlations was then independently

correlated to individual changes in depression and fatigue scores (both acute and long-term, where available), and peripheral inflammation markers (for plasma samples acquired concomitantly with the fMRI data) using partial Spearman correlations where we also accounted for sex and age. FDR correction was applied for the total number of parameters tested in each dataset.

Results

Effects of interferon-α and anti-TNF treatments on mood, fatigue and peripheral cytokines

As reported previously(11), Interferon-α produced significant increases in depression scores at 4 weeks, but not 4h post-treatment. We found significant increases in fatigue ratings after interferon-α both at 4h and 4 weeks after treatment. Interferon-α administration resulted in significant increases in blood levels of IL-6, IL-10, IL-1 $R_{a,}$ but did not change the levels of TNF-α, 4h after treatment (Table 1). Anti-TNF treatment did not produce significant changes in depression scores at 24h or 12 weeks after treatment. However, it produced significant decreases in fatigue scores at 12 weeks, but not 24h, after treatment. Anti-TNF treatment resulted in decreased IL-6, IL-10, IL-1 $R_{a,}$ but did not change the levels of TNF-α, 4h after treatment (Table 1).

Global brain connectivity at baseline and after Interferon-α and anti-TNF

Brain maps depicting the regional distribution of GBC at baseline and after each treatment are shown in **Figure 2** and GBC changes (Post-administration > Baseline) for each treatment in **Figure 3** (see supplementary Table S1 and S2 for full statistics).

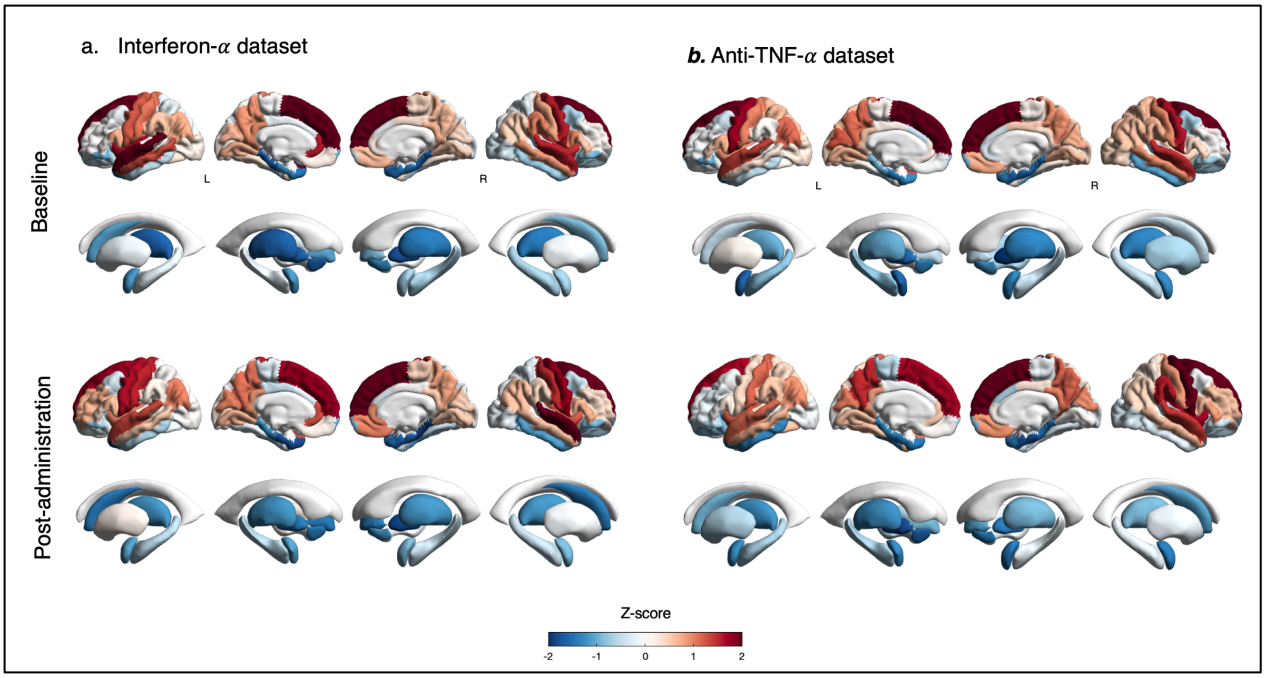

Figure 2. Global brain connectivity before and after each treatment. Regional distribution of global brain connectivity (GBC) for each cortical (upper row) and subcortical (lower row) region of the DK atlas. Colours depict z-scores. Positive (red) and negative (blue) z-scores indicate GBCs values above and below the mean GBC, respectively. (a) interferon-α dataset; (b) anti-TNF dataset. *Abbreviations*: L – Left; R – Right.

As illustrated in **Figure 3**, Interferon-α and anti-TNF induced discrete patterns of disturbance in GBC, both of which were dominated by decreases in GBC. Specifically, interferon-α induced small-to-medium sized decreases in regional GBC at the right supramarginal gyrus, right fusiform gyrus and left middle temporal gyrus at 4h post-administration ($p<0.05$, uncorrected) while anti-TNF induced acute medium decreases in regional GBC at the left caudate, left inferior temporal gyrus and left precentral gyrus at 24h post-administration ($p<0.05$, uncorrected). However, none of these individual changes survived FDR correction for multiple testing. Interestingly, spatial patterns of changes in GBC induced by interferon-α and anti-TNF treatments did not correlate or anti-correlate with each other ($r = -0.122$, $p_{spatial} = 0.271$) suggesting independent underlying processes.

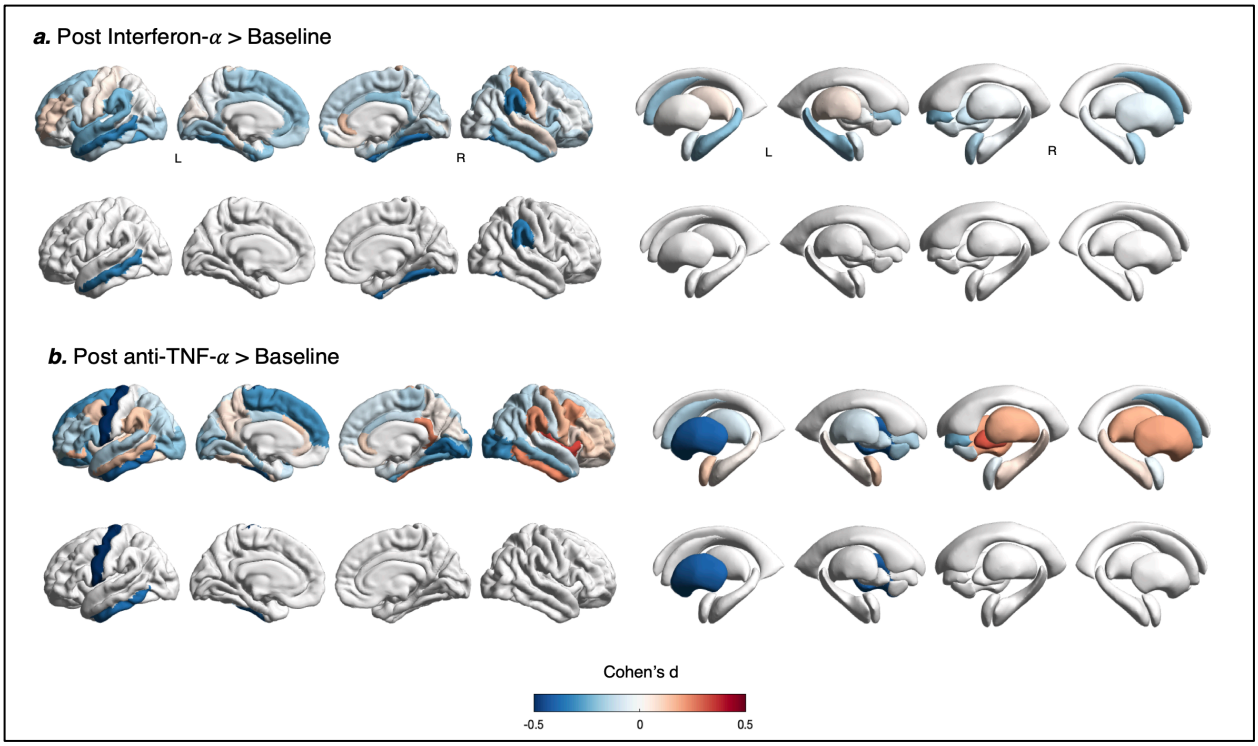

Figure 3. Effects of interferon-α and anti-TNF treatments on global brain connectivity. Brain maps depict the regional distribution of changes in global brain connectivity (GBC) in cortical and subcortical regions of the DK atlas after interferon-α (a) and anti-TNF (b) treatments compared to baseline. The upper row of each panel shows unthresholded Cohen's d effect sizes; the lower row all significant regions at p<0.05, uncorrected. No region survived FDR correction for the total number of regions tested within each dataset. *Abbreviations*: L – Left; R – Right.

Regional vulnerability to connectivity decreases after interferon-α and anti-TNF treatments can be captured by latent patterns of constitutive gene expression

For interferon-α, the first component (PLS_1) explained the highest proportion of GBC changes (23.32%) and was significantly positively correlated with regional changes in GBC after interferon-α (r = 0.483; $p_{spatial}$ = 0.006) (**Figure 4A**). For anti-TNF, the first component (PLS_1) explained the highest proportion of GBC changes (13.10%) and was positively correlated with regional changes in GBC after anti-TNF treatment (r = 0.362; $p_{spatial}$ = 0.023) (**Figure 4b**).

Of note, as treatment-induced changes in GBC were dominated by decreases, positive correlations between regional PLS_1 weights and GBC changes in both treatments mean that

negatively weighted genes are highly expressed in regions where GBC decreased the most but have low expression in regions where GBC had small or negligible increases. The reverse applies to genes with positive weights, which are highly expressed in regions where GBC had small or negligible increases and low expression in regions where GBC decreased the most. Hence, we focused our interpretation of the data on negatively weighted genes, which better captured the transcriptomic vulnerability concept we aimed to investigate.

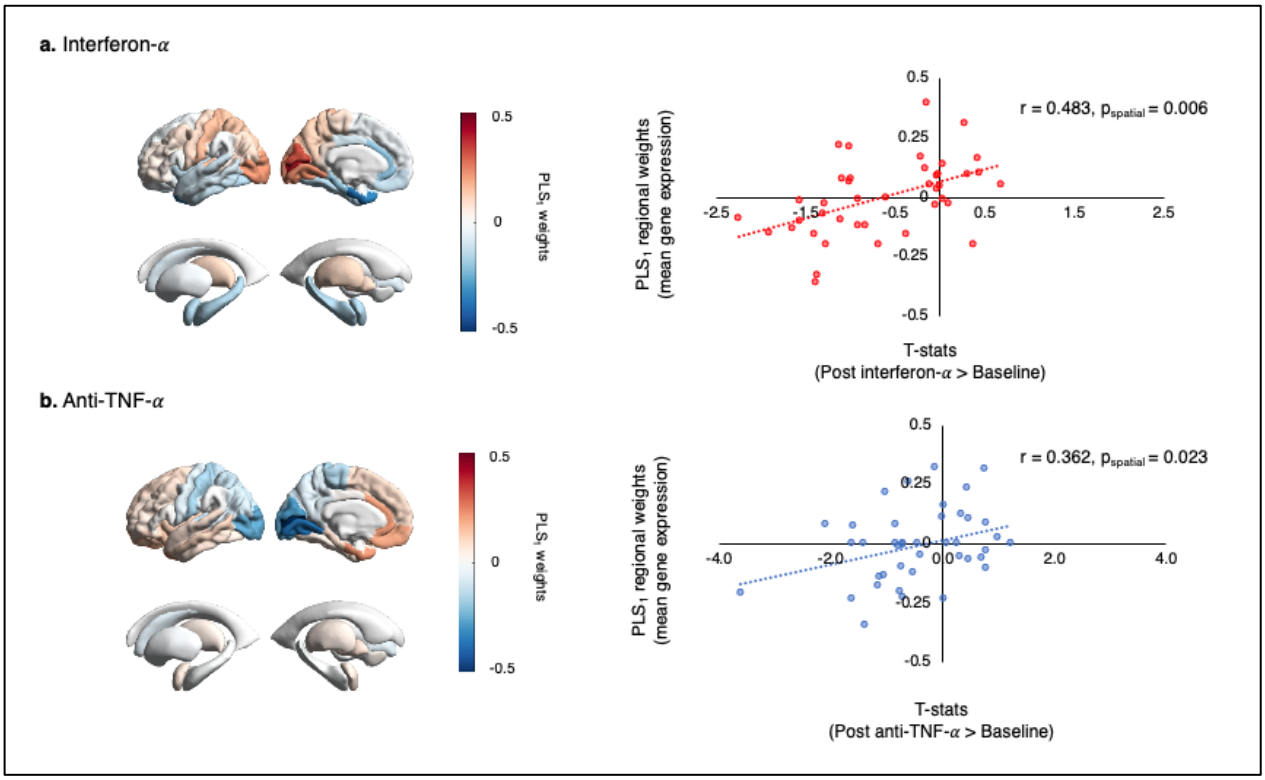

Figure 4. Transcriptomic regional vulnerability to connectivity decreases after interferon-α and anti-TNF. Brain maps on the left depict the regional distribution of PLS_1 weights across cortical and subcortical regions for the interferon-α (a) and anti-TNF (b) separately. Scatter plots on the right show positive correlations between the regional distribution of PLS_1 weights and the T-statistics quantifying treatment-induced changes in global brain connectivity in each dataset. Note: the T-statistics of treatment-induced changes in GBC reflect an average over the two brain hemispheres. *Abbreviations*: PLS – Partial Least Square.

Ensemble gene enrichment analyses identify divergent biological and cellular pathways underlying transcriptomic vulnerability to connectivity decreases induced by interferon-α and anti-TNF

For the interferon-α PLS_1 component, we observed significant enrichment for genes highly expressed in astrocytes, microglia and OPCs (all $p_{FDR}<0.05$) among those genes with negative weights with astrocytes being the strongest brain cell-type enrichment hit (**Figure 5a**; **SI Table S3**). We also identified significant enrichment for several gene ontology – biological pathway terms broadly related to neuroinflammation (**Figure 5b**, **SI Table S4**). *IFNAR1*, which encodes a protein that forms one of the two chains of the Type-I interferon membrane receptor was among the top negatively weighted genes (Z = -3.12, $p_{FDR}=0.004$, rank 14,847/15,633).

In contrast, for the anti-TNF-α PLS_1 component, we found significant enrichment for genes highly expressed in excitatory neurons ($p_{FDR}<0.05$) among those genes with negative weights (**Figure 5a; SI Table S5**). We also identified significant enrichment for several gene ontology – biological pathway terms broadly related to the synapse, including glutamatergic synaptic transmission (**Figure 5b**, **SI Table S6**). However, among the many genes of the TNF receptor superfamily sampled in the AHBA (*TNFRSF1A, 4, 8, 10A and B, 11A and B, 12A, 13C, 14, 21 and 25),* none showed significant association with GBC changes induced by anti-TNF treatment (all $p_{FDR}>0.05$).

Spatial alignment between individual connectivity changes and patterns of transcriptomic vulnerability correlates with inter-individual differences in peripheral inflammatory responses and depressive symptoms

In the Interferon-α dataset, the extent to which each participant expressed patterns of GBC changes aligning with the PLS_1 pattern of transcriptomic vulnerability negatively correlated with: i) increases in circulating IL-6, 4h after first interferon-α administration; ii) subsequent increases in HAM-D depression scores 4 weeks later (both $p_{FDR}<0.05$). None of the remaining correlations reached statistical significance (**Table 2**).

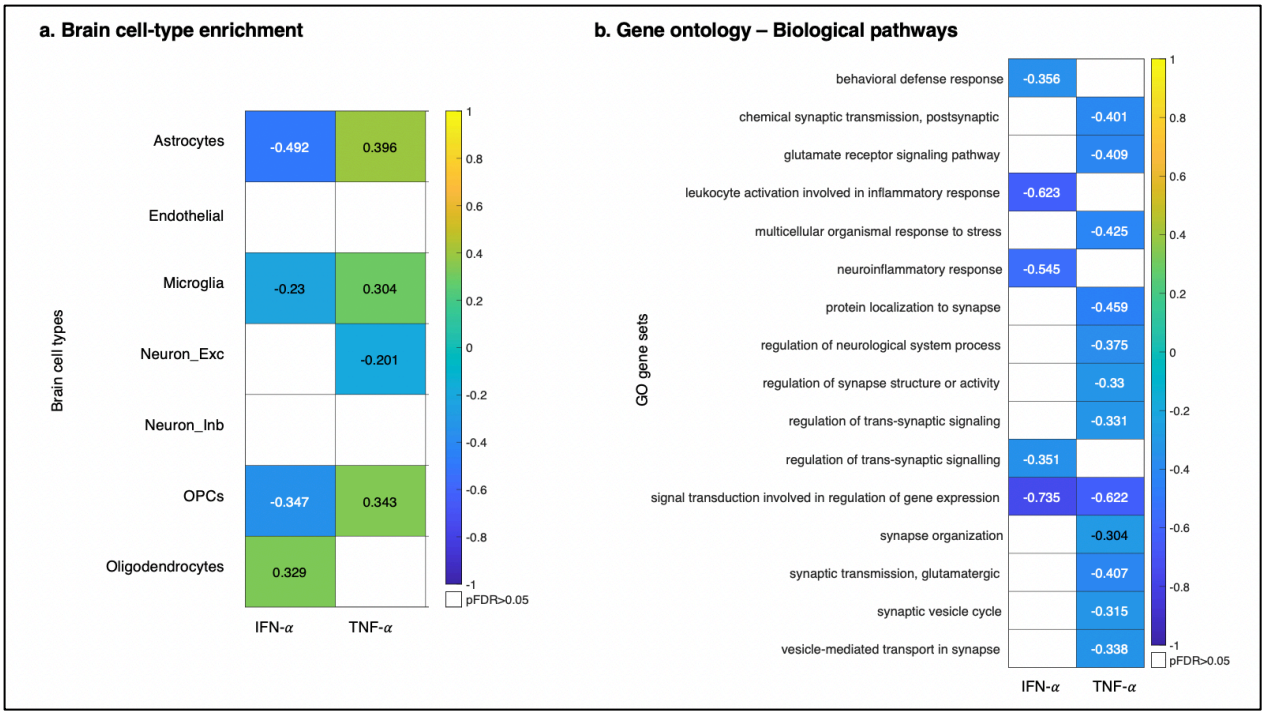

Figure 5. Ensemble gene set enrichment. The tile plots summarize the results of the gene set enrichment analyses on the ranked list of genes associated with global brain connectivity changes induced by interferon-α and anti-TNF: a. brain cell-type enrichment; b. enrichment for gene ontology (GO) – Biological pathways terms. Genes were ranked according to their respective weights in the first component of our partial least square regression models. Negative enrichment ratios indicate enrichment for a certain gene set among genes with negative weights. The reverse applies to positive enrichment ratios. The colour scale depicts enrichment ratio. Note: because we were predominantly interested in genes with high expression in regions where GBC decreases and low expression in regions with negligible GBC changes, we only interpreted enrichment for negatively weighted genes in both datasets. Abbreviations: Exc – excitatory; In – inhibitory.

In the anti-TNF dataset, the extent to which each subject expressed patterns of GBC changes aligning with the PLS_1 pattern of transcriptomic vulnerability positively correlated with peripheral decreases in IL-6, 24h after first anti-TNF treatment administration ($p<0.05$, uncorrected), though this correlation did not survive FDR correction for multiple testing. None of the remaining correlations reached statistical significance (**Table 3**).

Discussion

Our study contributes three key insights regarding regional variability in the effects of pro- and anti-inflammatory treatments on brain function and how it might be shaped by the transcriptomic landscape of the human brain. First, we demonstrate that interferon-α and anti-TNF therapies induced differential small-to-medium size decreases in resting GBC within distinct sets of brain regions. Second, we show that the spatial patterns of these GBC decreases associated with interferon-α and anti-TNF can be captured by latent multivariate patterns of constitutive regional expression of genes respectively related to: i) neuroinflammation and glial cells; and ii) glutamatergic neurotransmission and excitatory neurons. Third, we provide evidence that the extent to which each participant expressed patterns of GBC changes aligning with these patterns of transcriptomic vulnerability correlated with treatment-induced changes in systemic IL-6 and (for interferon-α treated patients) could predict subsequent treatment-induced changes in depressive symptoms. These results advance our knowledge of the relationship between systemic inflammation and brain function, with relevance for understanding how bidirectional changes in peripheral inflammation may contribute to the development/resolution of psychopathology.

Changes in brain function at rest after pro- and anti-inflammatory treatments

We provide a detailed map of acute changes in resting GBC induced by interferon-α and anti-TNF. For both treatments, we found that changes in functional connectivity were dominated by small-to-medium sized decreases in the GBC of regions previously implicated in mediating the brain effects of inflammation, such as the temporal lobe and/or basal ganglia(15). Global brain connectivity (GBC) computes the connectivity of each region in the brain to all other brain regions then summarizes this in a single value. Consequently, areas of high GBC are highly functionally connected with other areas and likely play a key role in coordinating large-scale patterns of brain activity. Reductions in GBC, such as those observed in our current study, may therefore indicate decreased participation of these brain area in larger networks. These findings are consistent with our previous observation in a subset of this interferon-α sample, that interferon-α can rapidly induce a profound shift in whole brain network structure, impairing global functional connectivity and the efficiency of parallel information exchange(16).

In contrast to our initial hypotheses, the strongest changes in GBC did not collocate or diverge in direction between interferon-α and anti-TNF treatments. Indeed, the overall spatial pattern of changes in GBC associated with each treatment did not globally anti-correlate either suggesting independent underlying processes, a proposition further supported by our transcriptomic vulnerability analyses. On reflection, this finding is perhaps unsurprising given that both treatments have different mechanisms of action. For instance, interferon-α readily crosses the blood brain-barrier (BBB) to enter the tissue parenchyma (84) and has been shown to directly impact brain function including modulation of neuronal firing rates in rodent studies(56). In contrast, anti-TNF drugs do not cross the BBB and most likely influence the brain indirectly by modulating immune activity peripherally and crosstalk with the brain resident neuroinflammatory machinery(85). Nevertheless, we must also take into consideration that patients in our two cohorts had distinct pre-existent medical conditions (hepatitis C vs arthritis) and are not directly comparable for sociodemographic variables such as gender representation, which might have contributed to the lack of correlation between changes in GBC in each cohort.

Transcriptomic vulnerability to regional brain function changes after immunomodulation

We demonstrate that regional vulnerability to GBC changes induced by interferon-α and anti-TNF treatments can be captured by multivariate patterns of constitutive gene expression in the healthy post-mortem human brain. In particular, in line with our hypothesis we found that the extent to which a region decreases GBC in response to interferon-α could be predicted by the relative abundance of mRNA of genes involved in glial neuroinflammatory response. In other words, the functional changes induced by interferon-α respect the canonical architecture of the brain-resident neuroinflammatory machinery, which supports previous suggestions that the effects of peripheral inflammation on the brain might entail engagement of local neuroinflammatory systems(55). Interestingly, we also found that the *IFNAR1* gene, which encodes a membrane protein that forms one of the two chains of a receptor for interferon-α, was among the top genes most strongly anti-correlated with GBC changes induced by interferon-α treatment. Since interferon-α can cross the BBB(84), these two findings are compatible with the

idea that by reaching the brain directly interferon-α might engage its own receptor in glial cells (which have been shown to express receptors and respond functionally to interferon-α(86)) to promote local neuroinflammation. This idea is further supported by studies in rodents showing that intraperitoneal injection of even modest amounts of interferon-α rapidly induces interferon-sensitive genes within the brain(87), and other studies reporting increases in CSF interferon-α after systemic administration of interferon-α in both primates(88) and humans(89).

The pattern of transcriptomic vulnerability to GBC decreases after anti-TNF treatment was dominated by the spatial distribution of the expression of neuronal genes broadly related to glutamatergic neurotransmission and synaptic structure and function. Like interferon-α, TNF (but not anti-TNF drugs) can cross the blood-brain-barrier, though permeability is many times lower (90). However, in our current study among the many genes of the TNF receptor superfamily, none figured among the genes more negatively associated with GBC changes induced by anti-TNF treatment, which points towards signalling through other pathways. In line with this, a recent CSF proteomic analysis showed that anti-TNF therapy in patients with arthritis reduces CSF concentrations of a broad range of acute phase and immune response proteins(91).

The biological functions of TNF in the brain are yet to be fully understood (92), however our findings are broadly in line with previous studies demonstrating that TNF-α regulates synapse function by controlling neurotransmitter receptor trafficking and is a critical mediator of the process of homeostatic synaptic scaling(93). For instance, neurons respond to elevated levels of TNF by rapidly increasing excitatory synaptic strength and weakening inhibitory synaptic strength, resulting in a higher excitatory/inhibitory ratio(94). Specifically, TNF-α increases neuronal expression of the post-synaptic glutamatergic AMPA receptor resulting in a uniform increase to the strength of all synapses to the cell in response to prolonged changes in firing activity(94). TNF-α also increases glutamate neurotoxicity, an effect that is mediated by the glutamatergic NMDA and AMPA receptors(95). Toxic effects of inflammation-induced increases in extrasynaptic glutamate signaling have been suggested to play a key role in the disruptions of network integrity that are present in at least some patients with depression(96, 97). If TNF-α modulates brain

function primarily by impacting on synaptic function, then it is plausible that regions which are constitutively populated by higher numbers of neuronal cells might be more strongly impacted by anti-TNF treatment than other regions where the neuronal machinery is less abundant. Nevertheless, animal studies have also reported effects of systemic anti-TNF treatments on microglia activation(98). Hence, it is possible that anti-TNF treatments may also have smaller concomitant effects on neuroinflammatory cells which might not be strong enough to drive the macroscopic pattern of changes in brain function measured with fMRI.

Further corroborating the plausibility of the transcriptomic vulnerability models we describe, we demonstrate that the extent to which each subject physically expressed patterns of GBC changes aligning with these patterns of transcriptomic vulnerability moderately correlated with treatment-induced changes in systemic IL-6 and (for interferon-α) could predict later (4 weeks) changes in depressive symptoms. These findings are interesting since we also found that interferon-α and anti-TNF-α treatments produced acute increases and decreases, respectively, in IL-6. IL-6 is a soluble mediator with a pleiotropic effect on inflammation, which is promptly produced in response to infections and tissue injuries, contributes to host defence through the stimulation of acute phase responses, haematopoiesis, and immune reactions(99). IL-6 can cross the blood-brain-barrier and reach the brain through mediated transport(99), and plays a critical role in the pathogenesis of neuroinflammatory disorders and in the physiological homeostasis of neural tissue(100). Interestingly, associations between peripheral levels of circulating IL-6 and measures of brain's connectivity have been demonstrated in patients with MDD(101). Therefore, our findings corroborate our initial hypotheses and lend support to current models postulating that a crosstalk between the peripheral and brain immune systems might contribute to the changes in brain and behaviour observed after pro- and anti-inflammatory treatments.

Strengths and Limitations

The use of two complimentary patient groups initiating pro- (interferon-α) and anti- (anti-TNF) inflammatory therapies is a major strength of our study that enabled us to demonstrate that systemic inflammation can rapidly and differentially modulate brain function. Further, by

following these patients up over time we could investigate whether acute changes in brain connectivity scaled with development/resolution of depressive symptoms. However, the use of clinical groups also had inherent weaknesses. For instance, for clinical scheduling reasons we needed to complete this study in a clinical (1.5 T) MRI scanner. Our sample sizes were also relatively modest, limiting power to detect small effects in the context of stringent multiple comparison correction across the whole brain. Patients also had distinct pre-existing conditions that limit direct comparisons between cohorts and might have interacted with treatment to shape brain responses. Furthermore, ethically we could not include a placebo condition against which to compare the effects of both interferon-α anti-TNF treatments on GBC.

Further limitations arise from the fact that the whole-brain gene expression data derives from only six *post-mortem* adult brains (mean age = 43 y). Moreover, our transcriptomic vulnerability models are correlational by nature and future studies investigating whether concomitant manipulation of glial neuroinflammatory activity (i.e. through antagonism of the microglia colony-stimulating factor 1 receptor (CSF1R) signalling(102)) or glutamatergic neurotransmission might indeed impact on the effects of interferon-α and anti-TNF treatments on the brain and behaviour, respectively. Furthermore, the lack of divergence in GBC changes induced by each treatment was unexpected, given that the interferon-α and anti-TNF treatments modulated systemic inflammatory markers and behaviour in opposite directions(11). Though we have interpreted these findings as likely reflecting different underlying mechanisms it is also possible that this may also have been influenced by differences in the post-administration time we acquired the data (4h in the interferon-α dataset and 24h in the anti-TNF dataset) or even an interaction between treatment and the pre-existing conditions. Nevertheless, in line with previous studies, our work dovetails with the idea that changes in brain function associated with inflammation are not idle but respect a spatial pattern of regional vulnerability, which differ between interferon-α and anti-TNF treatments and might be underpinned by distinct biological pathways.

To conclude, we demonstrate that regional variability in two elements of the cellular and transcriptomic landscape of the brain (glial neuroinflammation and glutamatergic

neurotransmission) explain regional heterogeneity in the effects of bidirectional changes in peripheral inflammation on brain function. Our findings connect genes, biological pathways and *in vivo* imaging markers of the impact of inflammation on brain function to generate new hypotheses about how inflammation might contribute to the development/resolution of psychopathology through effects on the brain.

Acknowledgments: We would like to thank all volunteers contributing data to this study.

Funding: DM, OD, MV, FET and SCRM are supported by the NIHR Maudsley's Biomedical Research Centre at the South London and Maudsley NHS Trust. MF is funded by the European Research Council (ERC) under the European Union's Horizon 2020 research and innovation program (ERC Advanced Grant agreement No 694665: CoBCoM - Computational Brain Connectivity Mapping).

Competing interests: The authors declare no competing interests. This manuscript represents independent research.

Tables and figures

Table 1. Mood, fatigue and cytokine response to interferon-α and anti-TNF treatments. Data represent mean ± standard deviation. [a]Values denote Hospital Anxiety and Depression Rating Scale (Depression component) for Inflammatory Arthritis and Hamilton Depression Rating Scale for Hepatitis-C patients; [b]Post-hoc comparison between baseline and second time-point (Sidak corrected); [c]Post-hoc comparison between baseline and last time-point (Sidak corrected).

	Arthritis (Baseline)	**Arthritis (24h)**	**Arthritis (12 weeks)**	**Statistics**	**Hepatitis-C (Baseline)**	**Hepatitis-C (4 hours)**	**Hepatitis-C (4 weeks)**	**Statistics**
Mood and Fatigue								
Depression scores[a]	6.35 (±3.20)	4.85 (±3.62)	5.05 (±3.66)	[b]0.071 [c]0.256	6.17 (±5.38)	6.57 (±6.55)	13.67 (±6.43)	[b]0.854 [c]<0.001
Fatigue Scores	68.75 (±18.88)	60.70 (±27.17)	44.35 (±26.57)	[b]0.189 [c]0.001	34.03 (±27.31)	46.00 (±28.63)	62.83 (±29.84)	[a]0.016 [b]<0.001
Peripheral cytokines								
IL-6	7.80 (±10.29)	3.89 (±5.92)	NA	0.042	1.42 (±1.03)	4.92 (±3.86)	NA	< 0.001
IL-10	0.36 (±0.83)	0.26 (±0.75)	NA	0.024	0.86 (±0.98)	1.46 (±1.49)	NA	0.017
TNF	0.76 (±1.98)	3.29 (±7.93)	NA	0.189	2.40 (±2.06)	2.36 (±1.77)	NA	0.903
IL-1 R_a	593.59 (±992.46)	451.22 (±976.23)	NA	0.017	168.61 (±136.51)	575.43 (±640.21)	NA	0.003

Table 2. Correlations with changes in peripheral inflammation markers and symptoms in the interferon-α dataset. Summary of correlations between the extent to which each subject manifests the spatial pattern of the first component of our partial least square regression model (PLS_1) in their pattern of global brain connectivity changes induced by interferon-α and changes in depression, fatigue and peripheral inflammatory markers. We used partial spearman

correlations, which accounted for sex and age. Both uncorrected and FDR corrected p-values are reported. Note that for the peripheral inflammation markers we used only data from samples acquired concomitantly with the fMRI data to maximize comparability. Abbreviations: HMA-D - Hamilton Depression Rating Scale.

	Clinical variable	**Statistics**	**PLS_1**
Depression and fatigue	**Δ**HMA-D (4h)	Rho	-0.116
		p (p_{FDR})	0.568 (0.745)
	ΔHMA-D (4 weeks)	Rho	-0.489
		p (p_{FDR})	0.009 (0.036)
	ΔFatigue (4h)	Rho	0.085
		p (p_{FDR})	0.652 (0.745)
	ΔFatigue (4 weeks)	Rho	0.253
		p (p_{FDR})	0.200 (0.533)
Peripheral inflammation markers	**Δ**IL_6 (4h)	Rho	-0.561
		p (p_{FDR})	0.005 (0.036)
	ΔIL_{10} (4h)	Rho	-0.125
		p (p_{FDR})	0.595 (0.745)
	ΔTNF (4h)	Rho	-0.074
		p (p_{FDR})	0.599 (0.745)
	ΔIL_1Ra (4h)	Rho	0.092
		p (p_{FDR})	0.781 (0.781)

Table 3. Correlations with changes in peripheral inflammation markers and symptoms in the anti-TNF dataset. Summary of correlations between the extent to which each subject manifests the spatial pattern of the first component of our partial least square regression model (PLS_1) in their pattern of global brain connectivity changes induced by the anti-TNF treatment and changes

in depression, fatigue, and peripheral inflammatory markers. We used partial spearman correlations, which accounted for sex and age. Both uncorrected p-values and p-values FDR corrected for multiple testing are reported. Note that for the peripheral inflammation markers we used only data from samples acquired concomitantly with the fMRI data to maximize comparability. Abbreviations: HADS - Hospital Anxiety and Depression Scale.

	Clinical variable	**Statistics**	**PLS_1**
Depression and fatigue	**Δ**HADS (24h)	Rho	-0.118
		p (p_{FDR})	0.662 (0.847)
	ΔFatigue (24h)	Rho	0.103
		p (p_{FDR})	0.706 (0.847)
Peripheral inflammation markers	**Δ**IL_6 (24h)	Rho	0.621
		p (p_{FDR})	0.009 (0.054)
	ΔIL_{10} (24h)	Rho	-0.246
		p (p_{FDR})	0.341 (0.847)
	ΔTNF (24h)	Rho	-0.145
		p (p_{FDR})	0.588 (0.847)
	ΔIL_1Ra (24h)	Rho	0.030
		p (p_{FDR})	0.889 (0.889)

References

1. Miller AH. Beyond depression: the expanding role of inflammation in psychiatric disorders. World Psychiatry. 2020;19(1):108-9.
2. Jeon SW, Yoon HK, Kim YK. Role of Inflammation in Psychiatric Disorders. Advances in experimental medicine and biology. 2019;1192:491-501.
3. Yuan N, Chen Y, Xia Y, Dai J, Liu C. Inflammation-related biomarkers in major psychiatric disorders: a cross-disorder assessment of reproducibility and specificity in 43 meta-analyses. Transl Psychiatry. 2019;9(1):233.
4. Reus GZ, Fries GR, Stertz L, Badawy M, Passos IC, Barichello T, et al. The role of inflammation and microglial activation in the pathophysiology of psychiatric disorders. Neuroscience. 2015;300:141-54.
5. Lee CH, Giuliani F. The Role of Inflammation in Depression and Fatigue. Front Immunol. 2019;10:1696.
6. Haapakoski R, Mathieu J, Ebmeier KP, Alenius H, Kivimaki M. Cumulative meta-analysis of interleukins 6 and 1beta, tumour necrosis factor alpha and C-reactive protein in patients with major depressive disorder. Brain, behavior, and immunity. 2015;49:206-15.
7. Levine J, Barak Y, Chengappa KN, Rapoport A, Rebey M, Barak V. Cerebrospinal cytokine levels in patients with acute depression. Neuropsychobiology. 1999;40(4):171-6.
8. Lindqvist D, Janelidze S, Hagell P, Erhardt S, Samuelsson M, Minthon L, et al. Interleukin-6 is elevated in the cerebrospinal fluid of suicide attempters and related to symptom severity. Biol Psychiatry. 2009;66(3):287-92.
9. Musselman DL, Lawson DH, Gumnick JF, Manatunga AK, Penna S, Goodkin RS, et al. Paroxetine for the prevention of depression induced by high-dose interferon alfa. The New England journal of medicine. 2001;344(13):961-6.
10. Capuron L, Gumnick JF, Musselman DL, Lawson DH, Reemsnyder A, Nemeroff CB, et al. Neurobehavioral effects of interferon-alpha in cancer patients: phenomenology and paroxetine responsiveness of symptom dimensions. Neuropsychopharmacology. 2002;26(5):643-52.
11. Davies KA, Cooper E, Voon V, Tibble J, Cercignani M, Harrison NA. Interferon and anti-TNF therapies differentially modulate amygdala reactivity which predicts associated bidirectional changes in depressive symptoms. Mol Psychiatry. 2020.
12. Tyring S, Gottlieb A, Papp K, Gordon K, Leonardi C, Wang A, et al. Etanercept and clinical outcomes, fatigue, and depression in psoriasis: double-blind placebo-controlled randomised phase III trial. Lancet. 2006;367(9504):29-35.
13. Kappelmann N, Lewis G, Dantzer R, Jones PB, Khandaker GM. Antidepressant activity of anti-cytokine treatment: a systematic review and meta-analysis of clinical trials of chronic inflammatory conditions. Mol Psychiatry. 2018;23(2):335-43.
14. Raison CL, Rutherford RE, Woolwine BJ, Shuo C, Schettler P, Drake DF, et al. A randomized controlled trial of the tumor necrosis factor antagonist infliximab for treatment-resistant depression: the role of baseline inflammatory biomarkers. JAMA Psychiatry. 2013;70(1):31-41.
15. Kraynak TE, Marsland AL, Wager TD, Gianaros PJ. Functional neuroanatomy of peripheral inflammatory physiology: A meta-analysis of human neuroimaging studies. Neurosci Biobehav Rev. 2018;94:76-92.
16. Dipasquale O, Cooper EA, Tibble J, Voon V, Baglio F, Baselli G, et al. Interferon-alpha acutely impairs whole-brain functional connectivity network architecture - A preliminary study. Brain, behavior, and immunity. 2016;58:31-9.

17. Sharpley AL, Cooper CM, Williams C, Godlewska BR, Cowen PJ. Effects of typhoid vaccine on inflammation and sleep in healthy participants: a double-blind, placebo-controlled, crossover study. Psychopharmacology (Berl). 2016;233(18):3429-35.
18. Harrison NA, Brydon L, Walker C, Gray MA, Steptoe A, Critchley HD. Inflammation causes mood changes through alterations in subgenual cingulate activity and mesolimbic connectivity. Biol Psychiatry. 2009;66(5):407-14.
19. Labrenz F, Wrede K, Forsting M, Engler H, Schedlowski M, Elsenbruch S, et al. Alterations in functional connectivity of resting state networks during experimental endotoxemia - An exploratory study in healthy men. Brain, behavior, and immunity. 2016;54:17-26.
20. Fitzgerald PB, Laird AR, Maller J, Daskalakis ZJ. A meta-analytic study of changes in brain activation in depression. Hum Brain Mapp. 2008;29(6):683-95.
21. Palmer SM, Crewther SG, Carey LM, Team SP. A meta-analysis of changes in brain activity in clinical depression. Front Hum Neurosci. 2014;8:1045.
22. Gray JP, Muller VI, Eickhoff SB, Fox PT. Multimodal Abnormalities of Brain Structure and Function in Major Depressive Disorder: A Meta-Analysis of Neuroimaging Studies. The American journal of psychiatry. 2020;177(5):422-34.
23. Cassidy PJ, Radda GK. Molecular imaging perspectives. J R Soc Interface. 2005;2(3):133-44.
24. Shen EH, Overly CC, Jones AR. The Allen Human Brain Atlas: comprehensive gene expression mapping of the human brain. Trends Neurosci. 2012;35(12):711-4.
25. Rizzo G, Veronese M, Heckemann RA, Selvaraj S, Howes OD, Hammers A, et al. The predictive power of brain mRNA mappings for in vivo protein density: a positron emission tomography correlation study. J Cereb Blood Flow Metab. 2014;34(5):827-35.
26. Patel Y, Shin J, Drakesmith M, Evans J, Pausova Z, Paus T. Virtual histology of multi-modal magnetic resonance imaging of cerebral cortex in young men. Neuroimage. 2020;218:116968.
27. Patania A, Selvaggi P, Veronese M, Dipasquale O, Expert P, Petri G. Topological gene expression networks recapitulate brain anatomy and function. Netw Neurosci. 2019;3(3):744-62.
28. Romero-Garcia R, Whitaker KJ, Vasa F, Seidlitz J, Shinn M, Fonagy P, et al. Structural covariance networks are coupled to expression of genes enriched in supragranular layers of the human cortex. Neuroimage. 2018;171:256-67.
29. Shin J, French L, Xu T, Leonard G, Perron M, Pike GB, et al. Cell-Specific Gene-Expression Profiles and Cortical Thickness in the Human Brain. Cereb Cortex. 2018;28(9):3267-77.
30. Seidlitz J, Vasa F, Shinn M, Romero-Garcia R, Whitaker KJ, Vertes PE, et al. Morphometric Similarity Networks Detect Microscale Cortical Organization and Predict Inter-Individual Cognitive Variation. Neuron. 2018;97(1):231-47 e7.
31. Liu S, Seidlitz J, Blumenthal JD, Clasen LS, Raznahan A. Integrative structural, functional, and transcriptomic analyses of sex-biased brain organization in humans. Proc Natl Acad Sci U S A. 2020;117(31):18788-98.
32. Shen J, Yang B, Xie Z, Wu H, Zheng Z, Wang J, et al. Cell-Type-Specific Gene Modules Related to the Regional Homogeneity of Spontaneous Brain Activity and Their Associations With Common Brain Disorders. Front Neurosci. 2021;15:639527.
33. Tang J, Su Q, Zhang X, Qin W, Liu H, Liang M, et al. Brain Gene Expression Pattern Correlated with the Differential Brain Activation by Pain and Touch in Humans. Cereb Cortex. 2021.

34. Zhu D, Yuan T, Gao J, Xu Q, Xue K, Zhu W, et al. Correlation between cortical gene expression and resting-state functional network centrality in healthy young adults. Hum Brain Mapp. 2021;42(7):2236-49.
35. Hansen JY, Markello RD, Vogel JW, Seidlitz J, Bzdok D, Misic B. Mapping gene transcription and neurocognition across human neocortex. Nat Hum Behav. 2021.
36. Wen J, Goyal MS, Astafiev SV, Raichle ME, Yablonskiy DA. Genetically defined cellular correlates of the baseline brain MRI signal. Proc Natl Acad Sci U S A. 2018;115(41):E9727-E36.
37. Diez I, Sepulcre J. Neurogenetic profiles delineate large-scale connectivity dynamics of the human brain. Nat Commun. 2018;9(1):3876.
38. Richiardi J, Altmann A, Milazzo AC, Chang C, Chakravarty MM, Banaschewski T, et al. BRAIN NETWORKS. Correlated gene expression supports synchronous activity in brain networks. Science. 2015;348(6240):1241-4.
39. Martins D, Giacomel A, Williams SCR, Turkheimer F, Dipasquale O, Veronese M, et al. Imaging transcriptomics: Convergent cellular, transcriptomic, and molecular neuroimaging signatures in the healthy adult human brain. Cell Rep. 2021;37(13):110173.
40. Forsyth J, Mennigen E, Lin A, Sun D, Vajdi A, Kushan-Wells L, et al. Prioritizing Genetic Contributors to Cortical Alterations in 22q11.2 Deletion Syndrome Using Imaging Transcriptomics. Cereb Cortex. 2021.
41. Hess JL, Radonjic NV, Patak J, Glatt SJ, Faraone SV. Autophagy, apoptosis, and neurodevelopmental genes might underlie selective brain region vulnerability in attention-deficit/hyperactivity disorder. Mol Psychiatry. 2020.
42. Altmann A, Cash DM, Bocchetta M, Heller C, Reynolds R, Moore K, et al. Analysis of brain atrophy and local gene expression in genetic frontotemporal dementia. Brain Commun. 2020;2(2).
43. Ji Y, Zhang X, Wang Z, Qin W, Liu H, Xue K, et al. Genes associated with gray matter volume alterations in schizophrenia. Neuroimage. 2021;225:117526.
44. Anderson KM, Collins MA, Kong R, Fang K, Li J, He T, et al. Convergent molecular, cellular, and cortical neuroimaging signatures of major depressive disorder. Proc Natl Acad Sci U S A. 2020;117(40):25138-49.
45. Keo A, Mahfouz A, Ingrassia AMT, Meneboo JP, Villenet C, Mutez E, et al. Transcriptomic signatures of brain regional vulnerability to Parkinson's disease. Commun Biol. 2020;3(1):101.
46. Romero-Garcia R, Seidlitz J, Whitaker KJ, Morgan SE, Fonagy P, Dolan RJ, et al. Schizotypy-Related Magnetization of Cortex in Healthy Adolescence Is Colocated With Expression of Schizophrenia-Related Genes. Biol Psychiatry. 2020;88(3):248-59.
47. Morgan SE, Seidlitz J, Whitaker KJ, Romero-Garcia R, Clifton NE, Scarpazza C, et al. Cortical patterning of abnormal morphometric similarity in psychosis is associated with brain expression of schizophrenia-related genes. Proc Natl Acad Sci U S A. 2019;116(19):9604-9.
48. Li J, Seidlitz J, Suckling J, Fan F, Ji GJ, Meng Y, et al. Cortical structural differences in major depressive disorder correlate with cell type-specific transcriptional signatures. Nat Commun. 2021;12(1):1647.
49. Jimenez-Marin A, Diez I, Labayru G, Sistiaga A, Caballero MC, Andres-Benito P, et al. Transcriptional Signatures of Synaptic Vesicle Genes Define Myotonic Dystrophy Type I Neurodegeneration. Neuropathol Appl Neurobiol. 2021.
50. Seidlitz J, Nadig A, Liu S, Bethlehem RAI, Vertes PE, Morgan SE, et al. Transcriptomic and cellular decoding of regional brain vulnerability to neurogenetic disorders. Nat Commun. 2020;11(1):3358.

51. Parker N, Patel Y, Jackowski AP, Pan PM, Salum GA, Pausova Z, et al. Assessment of Neurobiological Mechanisms of Cortical Thinning During Childhood and Adolescence and Their Implications for Psychiatric Disorders. JAMA Psychiatry. 2020;77(11):1127-36.
52. Vasa F, Romero-Garcia R, Kitzbichler MG, Seidlitz J, Whitaker KJ, Vaghi MM, et al. Conservative and disruptive modes of adolescent change in human brain functional connectivity. Proc Natl Acad Sci U S A. 2020;117(6):3248-53.
53. Fenchel D, Dimitrova R, Seidlitz J, Robinson EC, Batalle D, Hutter J, et al. Development of Microstructural and Morphological Cortical Profiles in the Neonatal Brain. Cereb Cortex. 2020;30(11):5767-79.
54. Khalili-Mahani N, Rombouts SA, van Osch MJ, Duff EP, Carbonell F, Nickerson LD, et al. Biomarkers, designs, and interpretations of resting-state fMRI in translational pharmacological research: A review of state-of-the-Art, challenges, and opportunities for studying brain chemistry. Hum Brain Mapp. 2017;38(4):2276-325.
55. Miller AH, Raison CL. The role of inflammation in depression: from evolutionary imperative to modern treatment target. Nat Rev Immunol. 2016;16(1):22-34.
56. Dafny N, Prieto-Gomez B, Dong WQ, Reyes-Vazquez C. Interferon modulates neuronal activity recorded from the hypothalamus, thalamus, hippocampus, amygdala and the somatosensory cortex. Brain Res. 1996;734(1-2):269-74.
57. Dowell NG, Cooper EA, Tibble J, Voon V, Critchley HD, Cercignani M, et al. Acute Changes in Striatal Microstructure Predict the Development of Interferon-Alpha Induced Fatigue. Biol Psychiatry. 2016;79(4):320-8.
58. Hess A, Axmann R, Rech J, Finzel S, Heindl C, Kreitz S, et al. Blockade of TNF-alpha rapidly inhibits pain responses in the central nervous system. Proc Natl Acad Sci U S A. 2011;108(9):3731-6.
59. Capuron L, Raison CL, Musselman DL, Lawson DH, Nemeroff CB, Miller AH. Association of exaggerated HPA axis response to the initial injection of interferon-alpha with development of depression during interferon-alpha therapy. Am J Psychiatry. 2003;160(7):1342-5.
60. Jenkinson M, Bannister P, Brady M, Smith S. Improved optimization for the robust and accurate linear registration and motion correction of brain images. Neuroimage. 2002;17(2):825-41.
61. Smith SM. Fast robust automated brain extraction. Hum Brain Mapp. 2002;17(3):143-55.
62. Pruim RH, Mennes M, van Rooij D, Llera A, Buitelaar JK, Beckmann CF. ICA-AROMA: A robust ICA-based strategy for removing motion artifacts from fMRI data. Neuroimage. 2015;112:267-77.
63. Avants BB, Tustison NJ, Song G, Cook PA, Klein A, Gee JC. A reproducible evaluation of ANTs similarity metric performance in brain image registration. Neuroimage. 2011;54(3):2033-44.
64. Preller KH, Duerler P, Burt JB, Ji JL, Adkinson B, Stampfli P, et al. Psilocybin Induces Time-Dependent Changes in Global Functional Connectivity. Biol Psychiatry. 2020;88(2):197-207.
65. Frigo MG. Global Functional Connectivity in Python. 2021.
66. Desikan RS, Segonne F, Fischl B, Quinn BT, Dickerson BC, Blacker D, et al. An automated labeling system for subdividing the human cerebral cortex on MRI scans into gyral based regions of interest. Neuroimage. 2006;31(3):968-80.
67. Cole MW, Yarkoni T, Repovs G, Anticevic A, Braver TS. Global connectivity of prefrontal cortex predicts cognitive control and intelligence. J Neurosci. 2012;32(26):8988-99.

68. Murphy K, Birn RM, Handwerker DA, Jones TB, Bandettini PA. The impact of global signal regression on resting state correlations: are anti-correlated networks introduced? Neuroimage. 2009;44(3):893-905.
69. Fox MD, Zhang D, Snyder AZ, Raichle ME. The global signal and observed anticorrelated resting state brain networks. J Neurophysiol. 2009;101(6):3270-83.
70. Hawrylycz MJ, Lein ES, Guillozet-Bongaarts AL, Shen EH, Ng L, Miller JA, et al. An anatomically comprehensive atlas of the adult human brain transcriptome. Nature. 2012;489(7416):391-9.
71. Arnatkeviciute A, Fulcher BD, Fornito A. A practical guide to linking brain-wide gene expression and neuroimaging data. Neuroimage. 2019;189:353-67.
72. Hawrylycz M, Miller JA, Menon V, Feng D, Dolbeare T, Guillozet-Bongaarts AL, et al. Canonical genetic signatures of the adult human brain. Nat Neurosci. 2015;18(12):1832-44.
73. Whitaker KJ, Vertes PE, Romero-Garcia R, Vasa F, Moutoussis M, Prabhu G, et al. Adolescence is associated with genomically patterned consolidation of the hubs of the human brain connectome. Proc Natl Acad Sci U S A. 2016;113(32):9105-10.
74. Zhang Y, Sloan SA, Clarke LE, Caneda C, Plaza CA, Blumenthal PD, et al. Purification and Characterization of Progenitor and Mature Human Astrocytes Reveals Transcriptional and Functional Differences with Mouse. Neuron. 2016;89(1):37-53.
75. Lake BB, Chen S, Sos BC, Fan J, Kaeser GE, Yung YC, et al. Integrative single-cell analysis of transcriptional and epigenetic states in the human adult brain. Nat Biotechnol. 2018;36(1):70-80.
76. Habib N, Avraham-Davidi I, Basu A, Burks T, Shekhar K, Hofree M, et al. Massively parallel single-nucleus RNA-seq with DroNc-seq. Nat Methods. 2017;14(10):955-8.
77. Darmanis S, Sloan SA, Zhang Y, Enge M, Caneda C, Shuer LM, et al. A survey of human brain transcriptome diversity at the single cell level. Proc Natl Acad Sci U S A. 2015;112(23):7285-90.
78. Li M, Santpere G, Imamura Kawasawa Y, Evgrafov OV, Gulden FO, Pochareddy S, et al. Integrative functional genomic analysis of human brain development and neuropsychiatric risks. Science. 2018;362(6420).
79. Fulcher BD, Arnatkeviciute A, Fornito A. Overcoming false-positive gene-category enrichment in the analysis of spatially resolved transcriptomic brain atlas data. Nat Commun. 2021;12(1):2669.
80. Alexander-Bloch A, Giedd JN, Bullmore E. Imaging structural co-variance between human brain regions. Nat Rev Neurosci. 2013;14(5):322-36.
81. Alexander-Bloch A, Raznahan A, Bullmore E, Giedd J. The convergence of maturational change and structural covariance in human cortical networks. J Neurosci. 2013;33(7):2889-99.
82. Vasa F, Seidlitz J, Romero-Garcia R, Whitaker KJ, Rosenthal G, Vertes PE, et al. Adolescent Tuning of Association Cortex in Human Structural Brain Networks. Cereb Cortex. 2018;28(1):281-94.
83. Markello RD, Misic B. Comparing spatial null models for brain maps. Neuroimage. 2021;236:118052.
84. Smith RA, Norris F, Palmer D, Bernhardt L, Wills RJ. Distribution of alpha interferon in serum and cerebrospinal fluid after systemic administration. Clin Pharmacol Ther. 1985;37(1):85-8.
85. Campbell SJ, Jiang Y, Davis AE, Farrands R, Holbrook J, Leppert D, et al. Immunomodulatory effects of etanercept in a model of brain injury act through attenuation of the acute-phase response. J Neurochem. 2007;103(6):2245-55.

86. Welsch JC, Charvet B, Dussurgey S, Allatif O, Aurine N, Horvat B, et al. Type I Interferon Receptor Signaling Drives Selective Permissiveness of Astrocytes and Microglia to Measles Virus during Brain Infection. J Virol. 2019;93(13).
87. Wang J, Campbell IL, Zhang H. Systemic interferon-alpha regulates interferon-stimulated genes in the central nervous system. Mol Psychiatry. 2008;13(3):293-301.
88. Felger JC, Alagbe O, Hu F, Mook D, Freeman AA, Sanchez MM, et al. Effects of interferon-alpha on rhesus monkeys: a nonhuman primate model of cytokine-induced depression. Biol Psychiatry. 2007;62(11):1324-33.
89. Raison CL, Dantzer R, Kelley KW, Lawson MA, Woolwine BJ, Vogt G, et al. CSF concentrations of brain tryptophan and kynurenines during immune stimulation with IFN-alpha: relationship to CNS immune responses and depression. Mol Psychiatry. 2010;15(4):393-403.
90. Pardridge WM. Biologic TNFalpha-inhibitors that cross the human blood-brain barrier. Bioeng Bugs. 2010;1(4):231-4.
91. Estelius J, Lengqvist J, Ossipova E, Idborg H, Le Maitre E, Andersson MLA, et al. Mass spectrometry-based analysis of cerebrospinal fluid from arthritis patients-immune-related candidate proteins affected by TNF blocking treatment. Arthritis Res Ther. 2019;21(1):60.
92. McCoy MK, Tansey MG. TNF signaling inhibition in the CNS: implications for normal brain function and neurodegenerative disease. J Neuroinflammation. 2008;5:45.
93. Santello M, Volterra A. TNFalpha in synaptic function: switching gears. Trends Neurosci. 2012;35(10):638-47.
94. Stellwagen D, Malenka RC. Synaptic scaling mediated by glial TNF-alpha. Nature. 2006;440(7087):1054-9.
95. Pickering M, Cumiskey D, O'Connor JJ. Actions of TNF-alpha on glutamatergic synaptic transmission in the central nervous system. Exp Physiol. 2005;90(5):663-70.
96. Haroon E, Chen X, Li Z, Patel T, Woolwine BJ, Hu XP, et al. Increased inflammation and brain glutamate define a subtype of depression with decreased regional homogeneity, impaired network integrity, and anhedonia. Transl Psychiatry. 2018;8(1):189.
97. Haroon E, Miller AH, Sanacora G. Inflammation, Glutamate, and Glia: A Trio of Trouble in Mood Disorders. Neuropsychopharmacology. 2017;42(1):193-215.
98. Clausen BH, Degn M, Martin NA, Couch Y, Karimi L, Ormhoj M, et al. Systemically administered anti-TNF therapy ameliorates functional outcomes after focal cerebral ischemia. J Neuroinflammation. 2014;11:203.
99. Tanaka T, Narazaki M, Kishimoto T. IL-6 in inflammation, immunity, and disease. Cold Spring Harb Perspect Biol. 2014;6(10):a016295.
100. Rothaug M, Becker-Pauly C, Rose-John S. The role of interleukin-6 signaling in nervous tissue. Biochim Biophys Acta. 2016;1863(6 Pt A):1218-27.
101. Aruldass AR, Kitzbichler MG, Morgan SE, Lim S, Lynall ME, Turner L, et al. Dysconnectivity of a brain functional network was associated with blood inflammatory markers in depression. Brain Behav Immun. 2021;98:299-309.
102. Hume DA, MacDonald KP. Therapeutic applications of macrophage colony-stimulating factor-1 (CSF-1) and antagonists of CSF-1 receptor (CSF-1R) signaling. Blood. 2012;119(8):1810-20.